

# Control-oriented Coupled Electrochemical Thermal Model for Li-Ion Batteries

Luca Onesto, Stefano Marelli, Matteo Corno

**Abstract**—This work proposes a numerical approach to the distributed modeling of electrochemical and thermal dynamics of Li-Ion batteries. The adopted approach enables an easy and scalable coupling of the classical pseudo 2D model with a spatially distributed thermal model. The partial differential equations are integrated using a finite difference method that gives rise to a set of Differential Algebraic Equations. The algebraic equations are dealt with a numerical approach based on closed-loop regulation of the voltage. This maintains the impedance causality of the battery model allowing for an easier integration in available simulation tools. This also enables to scale the approach at the battery level. Extensive simulations prove that proposed implementation can describe both the spatial features of Li-ion cells.

## I. INTRODUCTION

Li-ion batteries are the preferred choice for demanding applications from electric mobility to personal devices. They offer excellent energy and power density. These advantages come however at the cost of the need of advanced Battery Management Systems (BMS) [1].

BMSs continuously monitor the cells current, voltage, state of charge and temperature and make sure that they are within safe limits. In particular, thermal management of the cell is extremely important. If the cell temperature exceeds its maximum limit, a thermal runaway may happen that could result in an explosion [2]. Even without considering such extreme cases, the cell temperature has an impact on its degradation and ageing.

Current BMSs typically measure the surface temperature of the cells and the one of the cooling fluid [3], [4]. However, the temperature difference between the core and the surface of a Li-ion cell can reach high values [5]. With only the surface cell temperature available, BMSs need to adopt extremely conservative thermal management strategies that limit the performance of the cell. An accurate estimation of the cell temperature and its distribution could therefore improve safety and performance. In turns, such an accurate estimation requires accurate temperature models.

Over the years a number of thermal models have been developed for Li-ion cells [6], ranging from simple black-box models to extremely accurate CFD models. The available approaches can be classified in black-box, gray-box and white-box models. Black box methods describe the behavior of the cell without considering the physics phenomena that

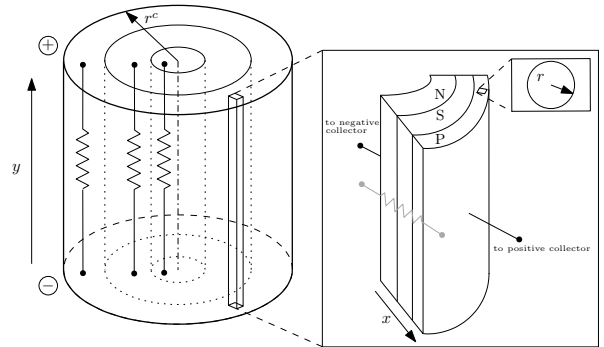


Fig. 1. Layout of a cylindrical Li-ion cell

determine the temperature. They tend to be simple and efficient, but lacks accuracy especially when used outside the conditions for which they have been identified. Gray-box models [7], [8] are usually based on electro-equivalent models that describe the cell electrical and thermal dynamics as a network of electrical elements (resistors, capacitors, voltage sources). They offer a good trade off between computational costs and accuracy, but they are unable to describe the temperature gradients inside the cell. Finally white-box models or electrochemical models are the most accurate. Among the available electrochemical models, the pseudo 2D model is now accepted as the standard one. In its original formulation [9], it does not account for the thermal dynamics; but in later works different approaches have been adopted. A family of approaches uses lumped thermal models, [5] develops a lumped-parameter thermal model. In [10], a reduced order model is obtained thanks to a polynomial approximation of the radial temperature distribution. This approach is based on the hypothesis that the heat generation is uniform. This hypothesis breaks under high discharge rate [11]. The above models are however not bidirectionally coupled, in the sense that the electrochemical process influence the heat generation, but the cell temperature does not impact the electrochemical reactions. This drawback is overcome in [12] and [13] where the classical pseudo 2D Electrochemical model of a cylindrical cell is coupled with a lumped thermal model, making the physiochemical properties of the cell temperature dependent. However, as explained before, a lumped thermal model, in certain operating conditions, may not be enough. Finally, there are works where the coupled electrochemical thermal model is solved through computational fluid dynamics, as in [14], or finite element solvers as in [15]. As affirmed in [16], these

This work was supported by MIUR SIR project RBSI14STHV

The authors are with the Dipartimento di Elettronica Informazione e Bioingegneria, Politecnico di Milano, via G. Ponzio 34/5, 20133, Milan, Italy.

Email: {luca.onesto | stefano.marelli | matteo.corno}@polimi.it

methods imply extensive computational resources, so they are not suited for applications.

This work proposes a control-oriented bidirectional coupled electrochemical thermal model for cylindrical Li-Ion cells (as the one depicted in 1).

The partial differential equation that arise from the mass, charge and energy conservation are discretized using a Finite Difference Method (FDM) applied to both electrochemical and the thermal dynamics. Thus, the model describes the spatial nature of both the electrochemical reactions and the heat generation. The spatial discretization of the electrochemical and the thermal models generates a set of Differential Algebraic Equation (DAE) which represents a finite number of impedances in parallel. This implies that the impedance causality that characterizes the P2D model is lost. In order to preserve this convenient feature (that is the basis of many estimation and control approaches in the literature), a closed-loop regulation of the voltage is developed.

Thus, the paper presents a numerical approach to solve the modeling and simulation of a finite number of P2D models in parallel accounting for their thermal coupling. The approximate approach exploits a frequency decoupling between the added closed-loop voltage regulation and the electrochemical dynamics. The advantages of the approach are multiple:

- 1) solving the closed-loop ODE is more computationally efficient than solving the original algebraic equations;
- 2) the integration of the model in commonly available signal-based simulation tools is easier;
- 3) the formulation is more easily applicable to classical control and estimation development techniques;
- 4) the formulation is scalable at the battery level.

The paper structure is as follows: Section II recalls the P2D model and discretizes it. Section III describes and discretizes the thermal dynamics. Section IV presents the numerical coupling approach. Section V validates the proposed approach comparing a number of simulations run in different conditions. Finally, this work takes end in Section VI.

## II. ELECTROCHEMICAL MODEL

Over the years, the literature has converged on the P2D model [9], [17], [18] as a good trade-off between complexity and accuracy. The model considers only the diffusion dynamics that take place across the battery film thickness,  $x$ , and the diffusion dynamics inside the spherical particles, along the *radial direction*  $r$  (see Figure 1).

Figure 2 summarizes the (continuous and discretized) conservation equations with the following nomenclature:  $c_s$  is the concentration of lithium in solid phase;  $c_e$  is the concentration of Li-ions in electrolyte phase;  $i_s$  is the electronic current in solid phase;  $i_e$  is the ionic current in electrolyte phase;  $\phi_s$  is the potential of solid phase;  $\phi_e$  is the potential of electrolyte phase.  $D_s$  is the solid phase diffusion coefficient;  $F$  is the Faraday's constant;  $a_s$  is the specific interfacial area of an electrode;  $D_e^{eff}$  is the effective diffusion coefficient;  $t_+^0$  is the transference number of Li+

Fig. 2. Electrochemical model equations.

(assumed as a constant);  $\sigma^{eff}$  is the effective conductivity;  $k^{eff}$  is the effective ionic conductivity, while  $k_D^{eff}$  is the effective diffusion conductivity. A few geometrical quantities are defined as well:  $A$  is the electrode plate area;  $\delta_{n,s,p}$ , are, respectively, the thickness of the negative and positive electrodes and separator;  $L = \delta_n + \delta_s + \delta_p$  is the overall film thickness.

The molar flux  $j^{Li}$  at the surface of active material particles is described by the *Butler-Volmer kinetics* equation:

$$j^{Li} = a_s j_0 \left[ \exp\left(\frac{\alpha_a F}{RT} \eta\right) - \exp\left(-\frac{\alpha_c F}{RT} \eta\right) \right] \quad (1)$$

where  $\alpha_{a,c}$  represents the anodic and cathodic transfer coefficients;  $R$  is the universal gas constant;  $T$  is the temperature;  $j_0$  is the exchange current density.  $\eta$  represents the reaction overpotential:

$$\eta = \phi_s - \phi_e - U(c_{se}). \quad (2)$$

The thermodynamic equilibrium potential  $U$  depends on the surface concentration  $c_{se}$  as described by [19] and not reported here for brevity's sake. The gradients of  $i_s$  and  $i_e$  depend on  $j^{Li}$ :

$$\frac{\partial i_s}{\partial x} = -j^{Li} \quad \frac{\partial i_e}{\partial x} = j^{Li};$$

satisfying the following constraints within the separator  $x \in [\delta_n, \delta_n + \delta_s]$ :

$$\frac{\partial i_s}{\partial x}(x) = \frac{\partial i_e}{\partial x}(x) = 0 \quad (3)$$

$$i_s(x) = 0 \quad (4)$$

$$i_e(x) = -k^{eff} \frac{\partial \phi_e}{\partial x} - k_D^{eff} \frac{\partial \ln(c_e)}{\partial x} = \frac{I}{A}. \quad (5)$$

The terminal cell voltage is:

$$V = \phi_s(x=L) - \phi_s(x=0) - \frac{R_f}{A} I \quad (6)$$

where  $R_f$  is the electrode surface film resistance. The P2D model is discretized as in [20]: the negative and positive electrodes and the separator are divided in the  $x$  direction in  $N_{n,s,p}$  elements and spacing  $\Delta x_{n,s,p}$ ; each spherical active material particle is divided, along its radius, in  $N_r$  sectors spaced  $\Delta r$ . This results in a total of  $(N_r + 1)(N_n + N_p) + N_s$  Ordinary Differential Equations (ODEs), and  $5(N_n + N_p) + 2N_s - 3$  non-linear algebraic constraints.

### III. THERMAL MODEL

The derivation of the thermal model is based on the fundamental hypothesis that the temperature gradient along the *axial direction*  $y$  is negligible ([11], [21]); as a consequence, the temperature dynamics are described by a 1D heat conduction in a cylinder:

$$\rho c_p \frac{\partial T}{\partial t} = k_t \frac{\partial^2 T}{\partial r^2} + \frac{k_t}{r^c} \frac{\partial T}{\partial r^c} + Q \quad (7)$$

with boundary conditions:

$$\left. \frac{\partial T}{\partial r^c} \right|_{r^c=0} = 0, \quad \left. \frac{\partial T}{\partial r^c} \right|_{r^c=R^c} = -\frac{h}{k_t} (T - T_\infty) \quad (8)$$

where  $T_\infty$  is the environment temperature, considered constant,  $k_t$  is the thermal conductivity,  $\rho$  is the density,  $h$  is the convection heat transfer coefficient,  $c_p$  is the specific heat capacity,  $Q$  is the volumetric heat generation rate,  $r^c$  and  $R^c$  are the radial direction and the radius of the cylinder, respectively. Considering an heterogeneous cylinder, the heat capacity  $C_p$  is calculated from the corresponding component values, as proposed in [22]:

$$C_p = \rho c_p = \sum_{i,k} \frac{\delta_i \varepsilon_{k,i} \rho_{k,i} c_{p,k,i}}{L} \quad (9)$$

where subscript  $k$  stands for the phase (solid or electrolyte) and subscript  $i$  stands for the component (n, s, p). In (9),  $\delta_i$  is the thickness of the  $i$ -th component and  $\varepsilon_k$  is the volume fraction of the  $k$ -th phase in the  $i$ -th component.  $Q$  is the sum of three terms: the volumetric reaction heat  $Q_j$ , the volumetric ohmic heat  $Q_o$ , the volumetric heat generated due contact resistance  $Q_f$ :

$$Q = Q_j + Q_o + Q_f$$

where

$$Q_j = \frac{1}{h^c} \int_0^L j^{Li} \eta dx, \quad Q_f = \frac{R_f}{h^c} \tilde{i}^2,$$

$$Q_o = \frac{1}{h^c} \int_0^L \sigma^{eff} \left( \frac{\partial \phi_s}{\partial x} \right)^2 + k^{eff} \left( \frac{\partial \phi_e}{\partial x} \right)^2 + k_D^{eff} \left( \frac{\partial \ln(c_e)}{\partial x} \right) \left( \frac{\partial \phi_e}{\partial x} \right) dx.$$

In the above expressions,  $h^c$  is the height of the cylinder and  $\tilde{i}$  is the specific current density. Note the dependency

on electrochemical variables; which determines the coupling between the two domains (thermal and electrochemical).

In analogy with the technique shown for the electrochemical model, the above PDEs are discretized with a finite difference method along the radial direction. The cell is thus divided in a finite number of elements ( $N_c$ ).

Two discretization approaches are considered: a constant radius and a constant-volume discretization. The constant radius approach divides the radius of the cell in with a constant step  $\Delta r^c = \frac{R^c}{N_c}$ ; the constant volume approach divides the cell in  $N_c$  subcells with the same volume. For brevity's sake, the following results refer to the constant-volume discretization only.

According to the FDM, (7) becomes:

$$\rho c_p \dot{T}_z = k_t \left[ \frac{T_{z-1} - 2T_z + T_{z+1}}{(\Delta r_z^c)^2} \right] + \frac{k_t}{r_z^c} \left[ \frac{T_{z+1} - T_z}{\Delta r_z^c} \right] + Q_z \quad (10)$$

where  $T_z$ ,  $r_z$ ,  $Q_z$  and  $V(k)$  are respectively the temperature, the radius and the heat generation rate of the  $z$ -th element. The term  $\Delta r_z^c$  is defined as:

$$\Delta r_z^c = r_z^c - r_{z-1}^c$$

where:

$$r_0^c = 0, \quad r_{N_c}^c = R^c$$

and the boundary conditions (8) become respectively:

$$T_1 - T_0 = 0, \quad \frac{T_{N_c+1} - T_{N_c}}{\Delta r_{N_c}^c} = -\frac{h}{k_t} (T_{N_c} - T_\infty).$$

### IV. COUPLED ELECTROCHEMICAL THERMAL MODEL

The previous sections show that the coupling between the electrochemical and thermal models is bidirectional, the thermal model depends on the heat generated by the chemical reaction; and the chemical reaction rates depend on the local temperature. In particular, the dependency of the electrochemical parameters on the temperature is well described by the Arrhenius equation:

$$\Psi(T) = \Psi_{ref} \left[ \frac{E_{act}^\Psi}{R} \left( \frac{1}{T_{ref}} - \frac{1}{T} \right) \right]$$

where  $\Psi$  is the generic parameter taken into account,  $\Psi_{ref}$  is the value of the parameter at the reference temperature  $T_{ref} = 25^\circ\text{C}$ ,  $R$  is the universal gas constant,  $E_{act}^\Psi$  is the activation energy of the physiochemical property. More specifically, the parameters that are considered temperature dependent are: the exchange current density  $i_0$ , the diffusion coefficient in the solid phase  $D_s$ , the diffusion coefficient in the electrolyte phase  $D_e$  and the electrolyte ionic conductivity  $K$ .

According to the FDM method described above, the Li-ion cell can be seen as set of  $N_c$  subcells in parallel, i.e. exhibiting the same output voltage, where each subcell is described by an electrochemical model and characterized by its own temperature (see Figure 1).

Thanks to the electrochemical model, it is possible to properly model the intercalation dynamics, as described in

Section II, and to calculate the heat generation rate  $Q_z$  of the  $z$ -th subcell as:

$$\begin{aligned}
Q_z &= Q_{j,z} + Q_{o,z} + Q_{f,z} \\
Q_{j,z} &= \frac{1}{h^c} \sum_i j_{i,z}^L \eta_{i,z} \Delta x \\
Q_{o,z} &= \frac{1}{h^c} \sum_i \left[ \sigma^{eff} \left( \frac{\phi_{s,i+1,z} - \phi_{s,i,z}}{\Delta x} \right)^2 \Delta x \right] \\
&\quad + \frac{1}{h^c} \sum_i \left[ k^{eff} \left( \frac{\phi_{e,i+1,z} - \phi_{e,i,z}}{\Delta x} \right)^2 \Delta x \right] \\
&\quad + \frac{1}{h^c} \sum_i \left[ k_D^{eff} \left( \frac{\ln(c_{e,i+1,z}) - \ln(c_{e,i,z})}{\Delta x} \right) \left( \frac{\phi_{e,i+1,z} - \phi_{e,i,z}}{\Delta x} \right) \Delta x \right] \\
Q_{f,z} &= \frac{R_f}{h^c A_z^2} (\hat{I}_z)^2
\end{aligned}$$

The term  $\hat{I}_z$  represents the input current of the  $z$ -th subcell. If the impedance of all the subcells is the same,  $\hat{I}_z$  is simply:

$$I_z = \frac{A_{Iz}}{A_l} I$$

where  $I$  and  $A_l$  are respectively the external current and the lateral surface area of the cell, while  $A_{Iz} = 2\pi r_z^c h^c$  is the lateral surface area of the  $z$ -th subcell. As the impedance of the subcells varies (due for example to temperature gradient in the cell) the current in each subcell may vary so that the voltage across the terminals of each subcell is the same (to guarantee the parallel nature of the connection).

The model is thus described by a set of  $N_c [(N_r + 1)(N_n + N_p) + N_s]$  ODEs and a set of  $N_c - 1$  constraint-type-equations, which represent the fact that the  $N_c$  subcells are in parallel:

$$V_{z+1} - V_z = 0 \quad \text{with} \quad z \in [1, N_c - 1]. \quad (11)$$

The coupling of the impedance-like causality of the P2D model with these constraints is not trivial. In other words, the discretization needed to account for the temperature gradient is not compatible with the impedance causality of the P2D model. Instead of changing the P2D model causality or explicitly accounting to the algebraic constraint, here a numerical approach is introduced. Each subcell is seen as a temperature and time dependent system that has, as input, the current density  $\hat{I}_z$  and, as output, the voltage  $V_z$ . A set of virtual controllers then distributes the current among the several subcell to guarantee that their voltage is maintained equal. Figure 3 graphically depicts the idea. The error  $e_z$ , defined as the difference between the voltage  $V_{z+1}$  and  $V_z$ , is the input of the regulator  $R_z$ , while its output is the control action  $u_z$ . The control action  $u_z$  changes the magnitude of the inputs  $\hat{I}_{z+1}$  and  $\hat{I}_z$ , according to the error  $e_z$ , in order to numerically force the Kirchhoff voltage equality. In other words, the proposed approach replaces (11) with a set of  $N_c - 1$  regulators that determine the total current distributions among the  $N_c$  impedances in parallel. The generic regulator  $R_z$  is a dynamical system described by  $N_b$  ODEs. This leads to a total of  $N_c [(N_r + 1)(N_n + N_p) + N_s] + N_b (N_c - 1) + N_c$  ODEs.

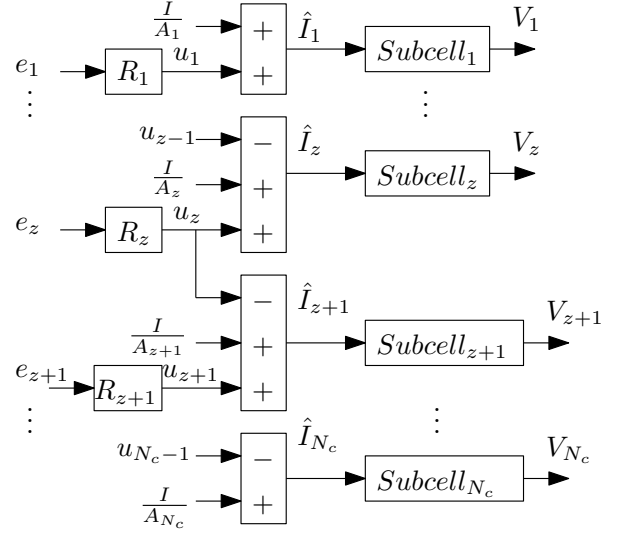


Fig. 3. Control-oriented coupled electrochemical thermal model layout.

The regulators are basically approximating the Kirchhoff law, as such the tuning of the regulators is particularly important. The regulators need to be tuned so that the  $e_z$ 's converge to zero with a dynamic faster than the electrochemical dynamics of interest. A trade-off arises: the faster the error dynamics is the stiffer and thus more computationally demanding the model is. This trade-off can also be employed as a calibration parameter that influence the simulation time.

Figure 4 plots the error dynamics during a 10C pulse discharge test with a starting temperature of  $T_\infty = 25^\circ\text{C}$ . From figure it is possible to see how the errors' magnitude

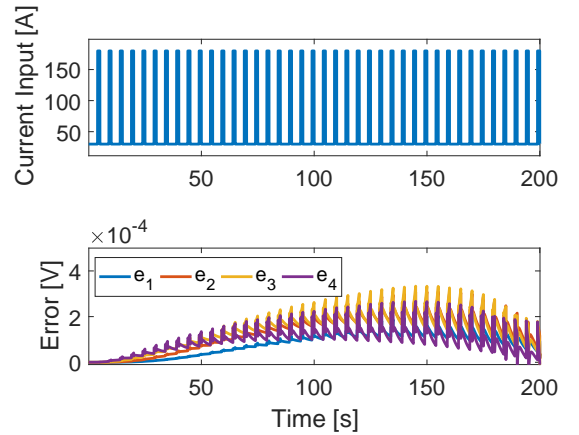


Fig. 4. Pulse train simulation of the coupled electrochemical thermal model; simulation time

is lower than  $5 \cdot 10^{-4}$  V.

## V. SIMULATION RESULTS

This section investigates the property of the proposed approach under realistic conditions. The model describes the 6Ah cell identified in [10], [12]. The current input  $I$  is calculated as the current requested in an HEV to a single Li-ion cell to perform a series of 4 US06 driving

cycles, for a total simulated time of 2403 s, where the mean and the maximum current are equal to 1 C and 25 C, respectively. The subcells' temperatures are initialized at the environment's one  $T_\infty = 25^\circ\text{C}$ . The heat transfer coefficient  $h$  is set to the value of  $60 \frac{\text{W}}{\text{m}^2\text{K}}$ .

In order to characterize the temperature behavior of the Li-ion cell, the following quantities are defined:

- The average temperature  $T_{bulk}$ :

$$T_{bulk} = \frac{\sum_{z=1}^{N_c} V_z^s \cdot T_z}{\sum_{z=1}^{N_c} V_z^s}$$

where  $V_z^s$  represents the volume of the  $z$ -th subcell.

- The index  $\Delta T$ , that summarizes the overall internal temperature difference:

$$\Delta T = T_1 - T_{N_c}$$

- The index  $\delta T$ , that summarizes the difference between the cell bulk temperature and the environment:

$$\delta T = T_{bulk} - T_\infty$$

- The index  $\mu$ , that quantifies the importance of considering the internal temperature gradient of the cell:

$$\mu = \frac{\Delta T}{\delta T} = \frac{T_1 - T_{N_c}}{T_{bulk} - T_\infty}$$

Figure 5 plots the values of the indexes at the end of the considered driving cycle, for different values of  $N_c$ , and the ratio  $\gamma$  between the simulation time and the simulated time. From figure, the following comments are due:

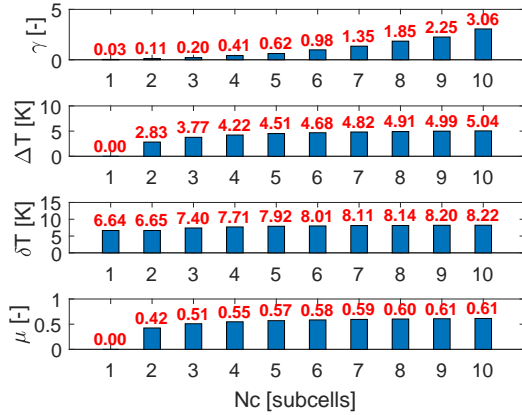


Fig. 5. Sensitivity analysis with respect to  $N_c$

- The values of the three indexes tend to converge as  $N_c$  increases.
- The computation time, while increasing more than linearly, can be kept at a faster than real time ratio. In particular a  $N_c = 6$  is selected.
- During the driving cycle, the internal temperature distribution is not negligible; this justifies the need for a coupled model.

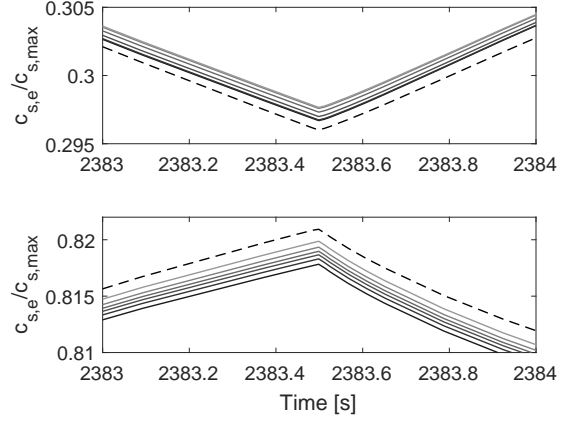


Fig. 6. Comparison of the concentrations dynamics.

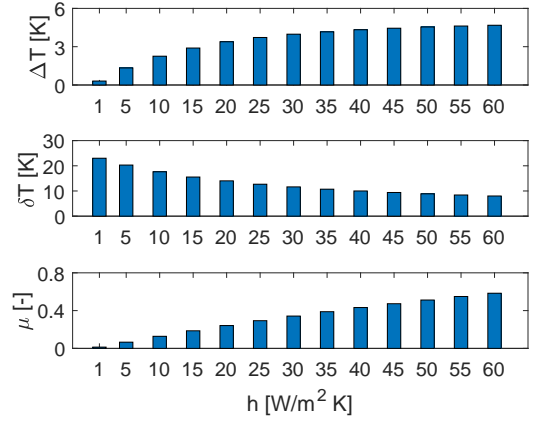


Fig. 7. Sensitivity analysis with respect to  $h$ .

Figure 6 provides a further demonstration of the importance of the coupled dynamics. It plots the comparison of the concentration dynamics in the outer element of the particle in the first element of the negative electrode (top subplot) and in the last element of the positive electrode (bottom subplot) for the case lumped thermal model ( $N_c = 1$  - dashed line) and of the distributed model ( $N_c = 6$  - solid line); the darkest solid line refers to the inner subcell, while the lighter solid line refers to the outer subcell. These results show that the temperature considerably affects the intercalation dynamics, therefore, if the internal temperature gradient is not negligible, the lithium concentration is not uniform along the radial direction  $r^c$ . As shown in Figure 6, the presented model provides  $N_c$  lithium concentrations with their related dynamics, that better describe the behavior of the cell with respect to the case of  $N_c = 1$ .

Finally, Figure 7 shows the results of a sensitivity analysis with respect to the heat transfer coefficient  $h$ . As expected, increasing  $h$ , the cell is exchanging heat (at the surface) more easily with the environment, so the temperature difference between the core and the surface of the cell increases, while the difference between the bulk temperature and the environment's one decreases. The index  $\mu$  increases as the

heat exchange coefficient grows. Hence, the greater is  $\mu$ , the more important is to consider the internal temperature gradient of the cell.

## VI. CONCLUSION

This work presents a numerical approach to couple the electrochemical and the thermal models of a cylindrical Li-ion cell. The approach is based on an approximation of the Kirchhoff law through a bank of voltage controllers that ensure the desired dynamics at the node. This approach is more flexible and easier to use than the formally correct solution of a system of algebraic differential equation.

The proposed model is extensively tested in simulation using a realistic driving cycle showing the impact of several parameters as well as the importance of considering the coupled distributed nature of the dynamics.

## REFERENCES

- [1] Paul WC Northrop, Bharatkumar Suthar, Venkatasailanathan Ramadesigan, Shriram Santhanagopalan, Richard D Braatz, and Venkat R Subramanian. Efficient simulation and reformulation of lithium-ion battery models for enabling electric transportation. *Journal of The Electrochemical Society*, 161(8):E3149–E3157, 2014.
- [2] Qingsong Wang, Ping Ping, Xuejuan Zhao, Guanquan Chu, Jinhua Sun, and Chunhua Chen. Thermal runaway caused fire and explosion of lithium ion battery. *Journal of Power Sources*, 208:210 – 224, 2012.
- [3] Robert R Richardson and David A Howey. Sensorless battery internal temperature estimation using a kalman filter with impedance measurement. *IEEE Transactions on Sustainable Energy*, 6(4):1190–1199, 2015.
- [4] Languang Lu, Xuebing Han, Jianqiu Li, Jianfeng Hua, and Minggao Ouyang. A review on the key issues for lithium-ion battery management in electric vehicles. *Journal of power sources*, 226:272–288, 2013.
- [5] Christophe Forgez, Dinh Vinh Do, Guy Friedrich, Mathieu Morcrette, and Charles Delacourt. Thermal modeling of a cylindrical lifepo 4/graphite lithium-ion battery. *Journal of Power Sources*, 195(9):2961–2968, 2010.
- [6] Gerardine G Botte, Venkat R Subramanian, and Ralph E White. Mathematical modeling of secondary lithium batteries. *Electrochimica Acta*, 45(15):2595–2609, 2000.
- [7] Long Lam, Pavol Bauer, and Erik Kelder. A practical circuit-based model for li-ion battery cells in electric vehicle applications. In *Telecommunications Energy Conference (INTELEC), 2011 IEEE 33rd International*, pages 1–9. IEEE, 2011.
- [8] M. Yazdanpour, P. Taheri, A. Mansouri, and B. Schweitzer. A circuit-based approach for electro-thermal modeling of lithium-ion batteries. In *2016 32nd Thermal Measurement, Modeling Management Symposium (SEMI-THERM)*, pages 113–127, March 2016.
- [9] Marc Doyle, Thomas F Fuller, and John Newman. Modeling of galvanostatic charge and discharge of the lithium/polymer/insertion cell. *Journal of the Electrochemical Society*, 140(6):1526–1533, 1993.
- [10] Youngki Kim, Jason B Siegel, and Anna G Stefanopoulou. A computationally efficient thermal model of cylindrical battery cells for the estimation of radially distributed temperatures. pages 698–703, 2013.
- [11] Said Al Hallaj, Hossein Maleki, Jong-Sung Hong, and J Robert Selman. Thermal modeling and design considerations of lithium-ion batteries. *Journal of Power Sources*, 83(1):1–8, 1999.
- [12] Kandler Smith and Chao-Yang Wang. Power and thermal characterization of a lithium-ion battery pack for hybrid-electric vehicles. *Journal of power sources*, 160(1):662–673, 2006.
- [13] Weifeng Fang, Ou Jung Kwon, and Chao-Yang Wang. Electrochemical-thermal modeling of automotive li-ion batteries and experimental validation using a three-electrode cell. *International journal of energy research*, 34(2):107–115, 2010.
- [14] CY Wang and Venkat Srinivasan. Computational battery dynamics (cbd)electrochemical/thermal coupled modeling and multi-scale modeling. *Journal of power sources*, 110(2):364–376, 2002.
- [15] Karthik Somasundaram, Erik Birgersson, and Arun Sadashiv Mujumdar. Thermal-electrochemical model for passive thermal management of a spiral-wound lithium-ion battery. *Journal of Power Sources*, 203:84–96, 2012.
- [16] Gi-Heon Kim, Ahmad Pesaran, and Robert Spotnitz. A three-dimensional thermal abuse model for lithium-ion cells. *Journal of Power Sources*, 170(2):476–489, 2007.
- [17] Kandler A Smith, Christopher D Rahn, and Chao-Yang Wang. Control oriented 1d electrochemical model of lithium ion battery. *Energy Conversion and management*, 48(9):2565–2578, 2007.
- [18] Adrien M. Bizeray, Shi Zhao, Stephen Duncan, and David A. Howey. Lithium-ion battery thermal-electrochemical model-based state estimation using orthogonal collocation and a modified extended kalman filter. *CoRR*, abs/1506.08689, 2015.
- [19] Kandler Smith and Chao-Yang Wang. Solid-state diffusion limitations on pulse operation of a lithium ion cell for hybrid electric vehicles. *Journal of Power Sources*, 161(1):628–639, 2006.
- [20] Matteo Corno, Nimitt Bhatt, Sergio M Savaresi, and Michel Verhaegen. Electrochemical model-based state of charge estimation for li-ion cells. *IEEE Transactions on Control Systems Technology*, 23(1):117–127, 2015.
- [21] TI Evans and Ralph E White. A thermal analysis of a spirally wound battery using a simple mathematical model. *Journal of The Electrochemical Society*, 136(8):2145–2152, 1989.
- [22] Sohel Anwar, Changfu Zou, and Chris Manzie. Distributed thermal-electrochemical modeling of a lithium-ion battery to study the effect of high charging rates. *IFAC Proceedings Volumes*, 47(3):6258–6263, 2014.